frontiers in Chemical Engineering

ORIGINAL RESEARCH
published: 18 October 2021
doi: 10.3389/fceng.2021.688498

Mechanical Stability Is Key for Large-Scale Implementation of Photocatalytic Surface-Attached Film Technologies in Water Treatment

*D.R. Ramos, M. Iazykov, M.I. Fernandez, J.A. Santaballa and M. Canle**

Universidade da Coruña, React! Group, Department of Chemistry, Faculty of Sciences & CICA, Coruña, Spain

Replacement of classical tertiary water treatment by chemical-free sunlight-driven photocatalytic units has been often proposed. Photocatalysts are required to be cost-effective, inert, chemically stable, reusable, and easy to separate and also that they are mechanically stable. The effect of mechanical stress on a photoactive TiO_2 layer, and on its effectivity for degradation of phenol as a model pollutant, has been studied during photocatalytic water treatment using NUV–vis light. Sol–gel (SG) and liquid phase deposition (LPD) methods have been used to coat spherical glass beads with the photocatalyst (TiO_2). Physicochemical characterization of coated glass beads has been performed by N_2 adsorption–desorption isotherms, SEM, EDXS, and AFM. Phenol photocatalyzed degradation was carried out both in stirred batch and flow reactors irradiated with a medium-pressure Hg-vapor lamp ($\lambda > 350$ nm). Phenol concentration was determined by HPLC, and its photoproducts were identified using HPLC/MS. In the stirred batch reactor, all LPD-coated glass beads displayed higher catalytic activity than SG-coated ones, which increased with calcination temperature, 700°C being the most efficient temperature. Preliminary etching of the glass beads surface yielded dissimilar results; whereas, phenol photodegradation with SG-coated etched glass beads is twice faster than with unetched SG ones, the rate reduces to one-third using LPD etched instead of unetched LPD glass beads. Phenol photodegradation using LPD is similar both in stirred batch and flow reactors, despite the latter uses a lower catalyst load. LPD-etched catalyst was recovered and reused in the stirred batch reactor; its activity reduced sharply after the first use, and it also lost activity in successive runs, ca. 10% of activity after each "use and recover" cycle. In the flow reactor, activity loss after the first experiment and recycling (ca. 30%) was much larger than in the following runs, where the activity remained rather constant through several cycles. LPD is more adequate than SG for TiO_2 immobilization onto glass beads, and their calcination at 700°C leads to relatively strong and reactive photocatalytic films. Still, TiO_2-coated glass beads exhibited very low photoactivity compared to TiO_2-P25 nanoparticles, though their separation is much easier and almost costless. The durability of the catalytic layer increases when using a flow reactor, with the pollutant solution flowing in a laminar regime through the photocatalyst bed. In this way, the abrasion of the photocatalytic surface is largely reduced and its photoactivity is better maintained.

Keywords: photocatalysis, supported photocatalyst, coating, flow photocatalysis, mechanical stability, heterogeneous photocatalysis

OPEN ACCESS

Edited by:
Martino Di Serio,
University of Naples Federico II, Italy

Reviewed by:
Claudio Imparato,
University of Naples Federico II, Italy
Pasi Tolvanen,
Abo Akademi University, Finland

****Correspondence:***
M. Canle
moises.canle@udc.es

Specialty section:
This article was submitted to Chemical Reaction Engineering, a section of the journal Frontiers in Chemical Engineering

Received: *30 March 2021*
Accepted: *05 August 2021*
Published: *18 October 2021*

Citation:
Ramos DR, Iazykov M, Fernandez MI, Santaballa JA and Canle M (2021) Mechanical Stability Is Key for Large-Scale Implementation of Photocatalytic Surface-Attached Film Technologies in Water Treatment. Front. Chem. Eng. 3:688498. doi: 10.3389/fceng.2021.688498

INTRODUCTION

The quest for new photocatalysts is often focused on obtaining compounds with increasingly higher catalytic activity. Frequently, the marketing prospects of the studied materials are considered as secondary in fundamental research. Thus, it is very common to find examples of applications of noble or rare metals (Ag-, Au-, Pt-, Ir-, etc.) that are doped onto or composited with different materials to produce highly efficient photocatalysts (Cao et al., 2020; Ibukun and Jeong, 2020; Meng et al., 2020; Xu et al., 2020) that may not be either sustainable or economically viable for most technological applications. Besides, the use of nanoparticles as catalysts is quite extended as the surface area increases when the particle size decreases, with the subsequent effect on efficiency for surface-based processes (Retamoso et al., 2019). Photocatalytic processes could be used for a variety of large-scale industrial or environmental applications as they offer a sustainable and economical alternative.

Water treatment, both for drinking and wastewater, is of utmost importance for human health, for environmental protection, and for the development of societies (General Assembly of the United Nations, 2015). Currently used water treatment processes are designed for the elimination of pathogenic microorganisms, not for the elimination of chemical pollution, including persistent and mobile organic chemicals (PMOCs). Among tertiary treatments, disinfection and the removal of undesired organic compounds can be mostly performed by chlorination or advanced oxidation processes (ozonation, photolysis, etc.) (White, 1986; Parsons, 2004). These processes might be effectively replaced by chemical-free, sunlight-driven photocatalytic units, provided photocatalysts become cost-effective, inert, and reusable. Therefore, used photocatalysts must be cheap, chemically stable, easy to separate, and, a frequently underestimated matter, mechanically stable. Apart from the price, two relevant physical properties, size and mechanical strength, must be taken into account in the choice of appropriate photocatalysts for water treatment.

The use of nanoparticles, despite their superior efficiency, must be discarded due to the economical restriction imposed by the need of nanofiltration to remove them, especially when dealing with huge volumes of water (Xi and Geissen, 2001). In this regard, thin film deposition techniques (Wang et al., 2014) applied on different surfaces have been proposed to allow a better catalyst recovery or even avoid this process. With respect to the critical concern on mechanical stability, these thin layers of photocatalysts are constantly exposed to hitting and abrasion, so only films with a high mechanical resistance would be appropriate for long repeated use under high flows.

The use of titanium dioxide (TiO_2) for water treatment applications is a benchmark due to its lack of toxicity, high stability under different conditions (pH, solvents, etc.), large abundance and inexpensiveness, and its suitability for degrading a broad range of pollutants (Lee et al., 1999; Senthilkumaar and Porkodi, 2005). The progress in the development of appropriate TiO_2 film deposition techniques is important to attain commercially applicable catalysts, although there are some other outstanding issues, such as the use of expensive and complex equipment, which hamper broad exploitation (Wang et al., 2014). Among thin film production methods, two relatively simple chemical solution deposition processes exhibit a high potential.

Sol–gel (SG) and liquid phase deposition (LPD) methods are the most promising techniques to coat glass substrates with TiO_2 layers (Yu et al., 2003; Xia et al., 2005; Gutiérrez-Tauste et al., 2006; Tasbihi et al., 2007; He et al., 2016). These two methods are reasonably fast, simple, and economical, although several unsuitable mechanical durability problems of the obtained films have been observed (Munafò et al., 2014; Goffredo and Munafò, 2015). Some authors have employed multilayer coatings to fix this issue by increasing film thickness and the hardness of the synthesized material (He et al., 2016). However, this procedure has not any real advantage, since adhesion between the film and substrate is usually stronger than interlayer cohesion, which leads to a straightforward peeling of the outer shell. Besides, these catalytic substrates have also been prepared with etching before coating the glass surface. This treatment has been performed in an attempt to improve the mechanical stability and recoverability of the supported photocatalyst.

Numerous studies have been published on photocatalytic TiO_2 films, mostly prepared by the SG method and supported on different glass substrates, such as beads (He et al., 2004), plates (Subba Rao et al., 2006; Štangar et al., 2006; Ćurković et al., 2014), fibers (Mikula et al. 1995), and others (Gartner et al., 2004; Singh et al., 2011; Ćurković et al., 2014), but also by the LPD method on glass beads (Shen et al., 2016) or plates (Ma et al., 2007; Kim et al., 2012; Liu et al., 2014). Besides, the resistance and durability of TiO_2 coatings have already been studied for different photocatalytic applications (Zainudin et al., 2010; Osborn et al., 2014; Calia et al., 2016). Here, we analyze the effect of mechanical stress on several photoactive TiO_2 coatings and their effectivity for phenol degradation during photocatalytic water treatment. Phenol has been selected as a pollutant model based on the common occurrence of phenol and phenolic compounds in natural, industrial, and domestic waste waters (Anku et al., 2017); their toxicity (Bruce et al., 2001) and considerable stability and persistence in aquatic environments (Wang et al., 2020); and the high number of articles that have discussed the photodegradation of phenol by several means over the last 20 years (Alemany et al., 1997; Dang et al., 2016). Etching of raw glass materials has also been performed in order to test its effect on both the photocatalytic activity of the TiO_2 surface and the stability of the coating. The obtained results reveal the upmost importance of mechanical stability for attaining the adequate recovering and recycling of the catalyst, a key aspect for the potential technological applicability of the prepared photocatalytic surfaces.

MATERIALS AND METHODS

Chemicals

Titanium (IV) butoxide (97%) and ammonium hexafluorotitanate (IV) (99%) from Sigma-Aldrich; boric acid

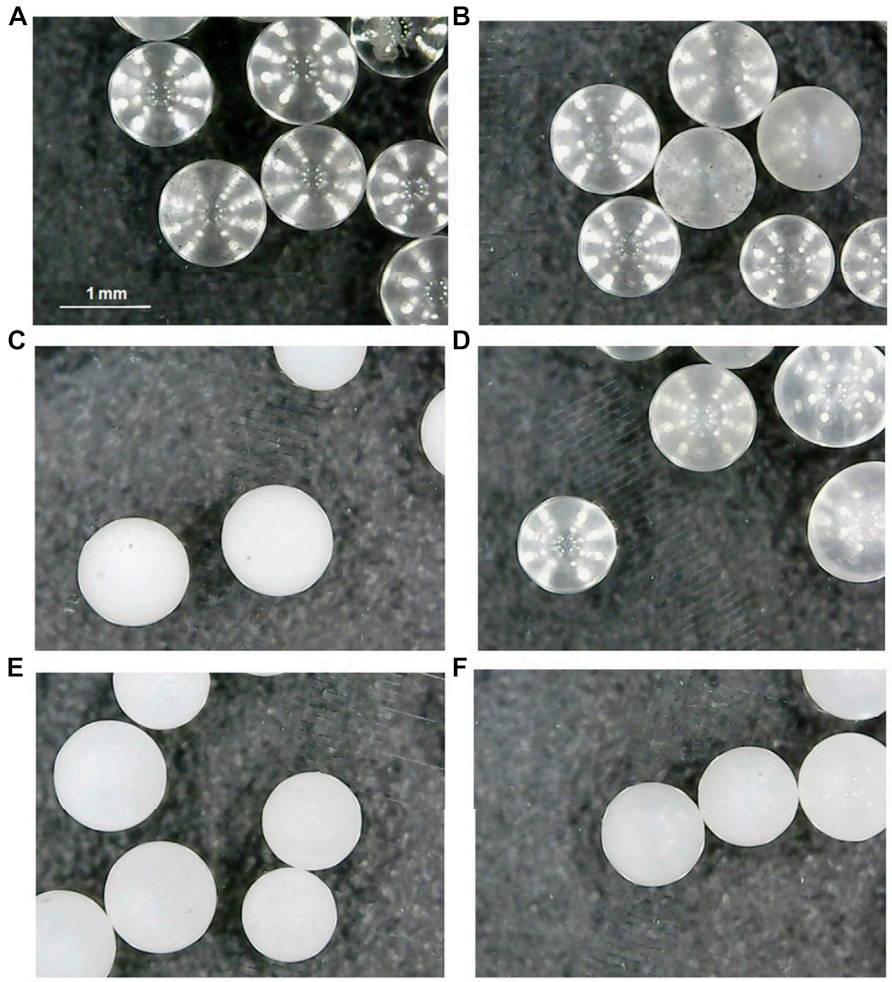

FIGURE 1 | Micrographs of the uncoated glass beads and the photocatalytic coated ones: **(A)** cleaned and **(b)** etched, uncoated glass beads; LPD-600 glass beads **(C)** before and **(D)** after two 6.5 h runs in a batch reactor; LPD-700 glass beads **(E)** before and **(F)** after 12 6.5 h runs in a flow reactor.

(99.5%) from Merck; nitric acid (65%), glacial acetic acid (99.5%), ethanol (99.5%), hydrochloric acid (37%), sodium hydrogen carbonate (p.a.), and acetone and phenol (98.5%) from PanReac AppliChem; commercial nanophotocatalyst TiO_2-P25 from Evonik; and diethanolamine (99%) from Fluka AG were used as received. ELIX-Q deionized water was employed to prepare solutions and for all other uses, but the mobile phase in HPLC measurements, where Milli-Q water was employed.

Glass beads (ca. 1.0 mm mean diameter) were purchased from Sigma-Aldrich and pretreated as in the following section.

Thin Film Deposition Techniques

Glass Pretreatment

Prior to TiO_2 deposition, glass beads were always cleaned by sonication, successively, in concentrated nitric acid, deionized water, and acetone and then air dried at 100°C (**Figure 1A**). Etching was carried out by immersion in a 0.5 mol L^{-1} aqueous $NaHCO_3$ solution and stored at 120°C for 20 h in an autoclave. The material was then washed with HCl and distilled water and then air dried at 100°C (**Figure 1B**) (Fujima et al., 2014).

Sol–Gel Method

TiO_2 coating was performed as proposed by Xia et al. (2005) and He et al. (2016). Titanium (IV) butoxide (14.2 ml) was added to ethanol (50 ml) with moderate magnetic stirring (300 rpm) for 10 min. Then, 1 ml of 0.1 mol L^{-1} HNO_3, 1 ml of water, and 1 ml of glacial acetic acid were sequentially added in drops, and the mixture was stirred at 300 rpm for 7 min to yield a pale-yellow gel. 25 g of glass beads were poured into the gel and stirred at 350 rpm for 15 min. This mixture was dried in the oven for 2 h at 105 °C. The obtained wrapped material was annealed in a muffle at 600°C.

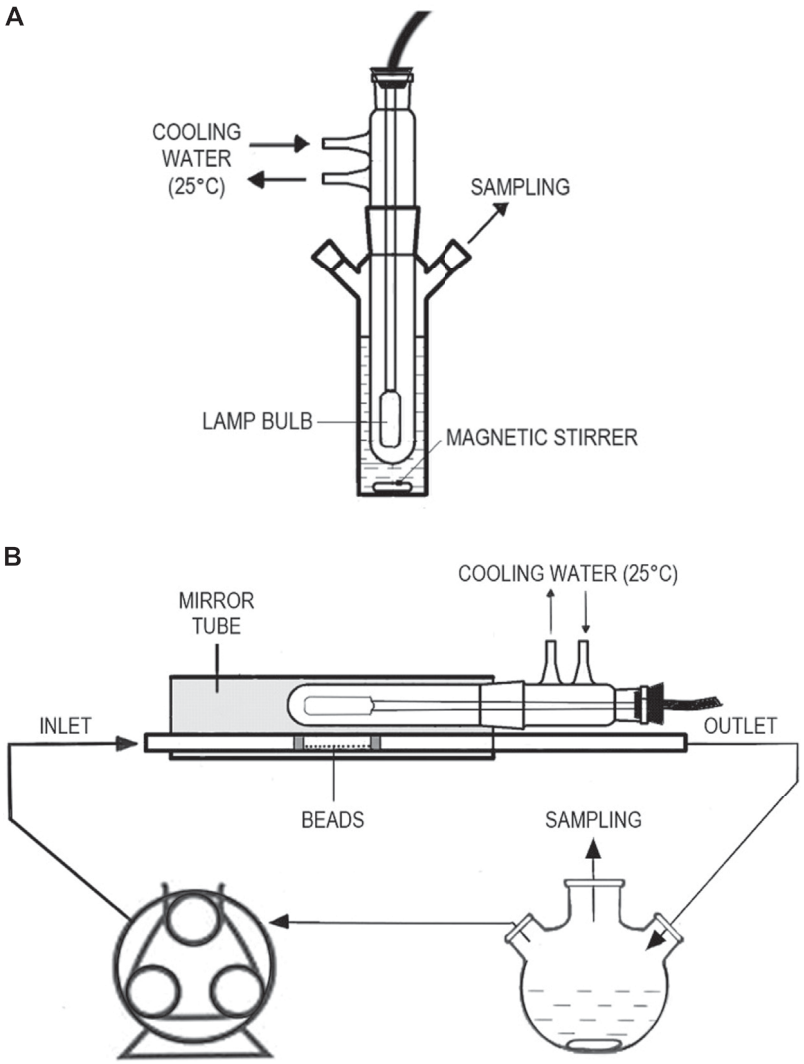

SCHEME 1 | Schematic representation of the photoreactors used in the study: **(A)** stirred batch reactor and **(B)** flow reactor.

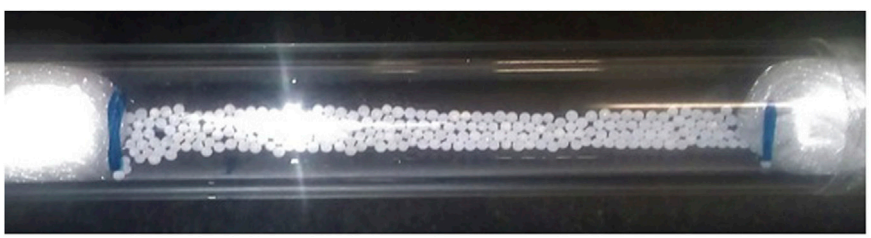

FIGURE 2 | 0.5 g of 1 mm (mean diameter) TiO_2-coated glass beads distributed on a borosilicate glass tube for flow-reactor photocatalysis experiments.

Liquid Phase Deposition Method

Glass beads were coated using the method proposed by Yu et al. (2003) and Gutiérrez-Tauste et al. (2006). Aqueous solutions of ammonium hexafluorotitanate and boric acid were mixed (final concentrations 0.1 and 0.3 mol L^{-1}, respectively) and stirred. The following equilibria take place:

$$[TiF_6]^{-2} + nH_2O \rightleftarrows [TiF_{6-n}(OH)_n]^{-2} + nHF \quad (1)$$

$$H_3BO_3 + 4HF \rightleftarrows HBF_4 + 3H_2O \quad (2)$$

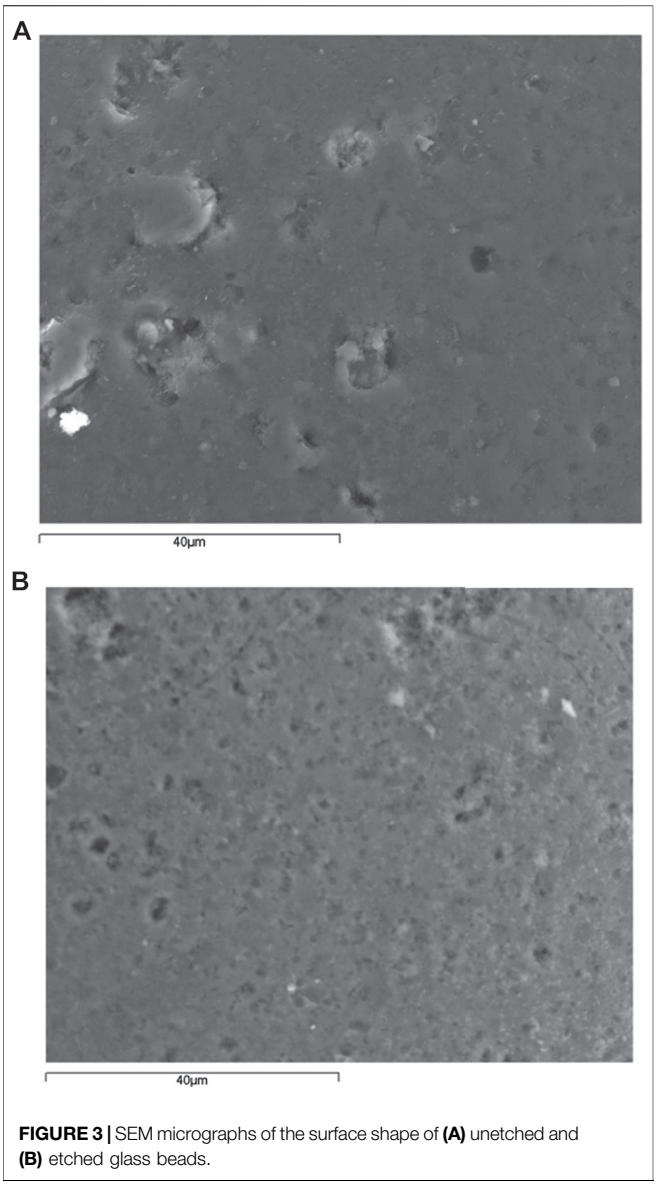

FIGURE 3 | SEM micrographs of the surface shape of **(A)** unetched and **(B)** etched glass beads.

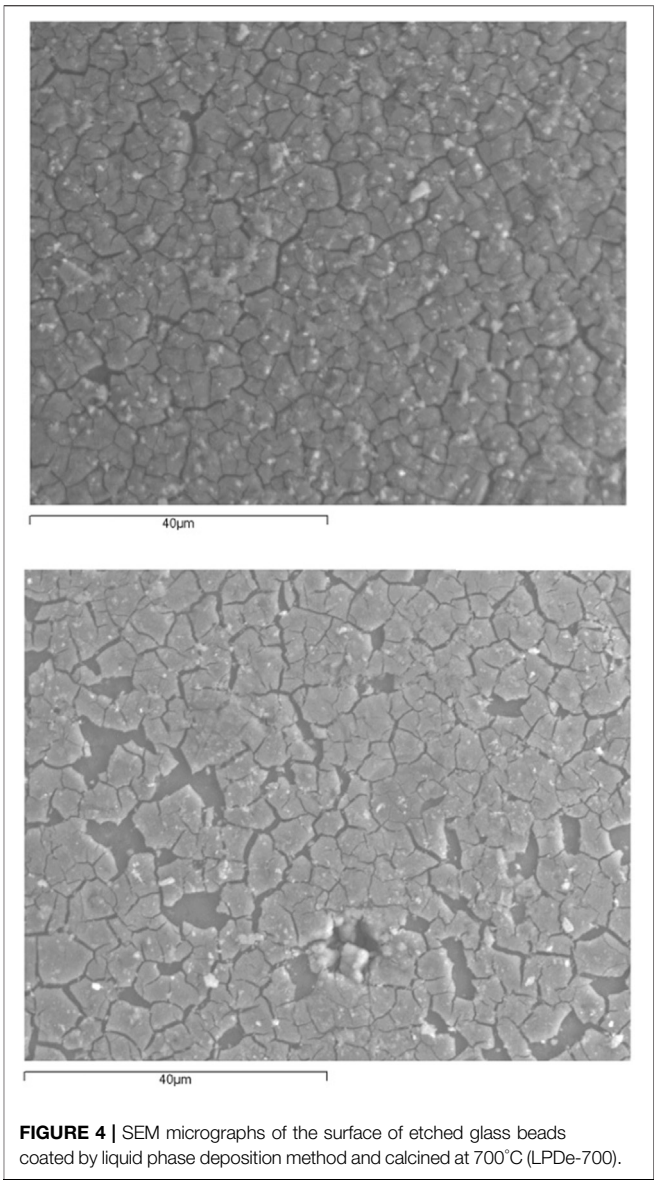

FIGURE 4 | SEM micrographs of the surface of etched glass beads coated by liquid phase deposition method and calcined at 700°C (LPDe-700).

The clean glass beads were dipped into this treatment solution and kept for 48 h at room temperature (ca. 20°C). The coated material was then washed with water, air dried at 100°C, and calcined at 500, 600, or 700°C.

Calcination

The furnace temperature was initially increased with a ramp rate of 3°C/min up to 100°C and held for 1 h. Then, the temperature was increased with the same ramp up to the final value and maintained for 1 h. At this point, the program was switched off and the calcined catalyst was allowed to cool down gradually to 32°C (overnight) inside the oven. The catalyst surface was then cleaned to remove any remaining powder or organic residue by rinsing with water and acetone. The obtained material is displayed in **Figures 1C,E**; no shape changes or deformations were apparent on the photocatalyst-coated glass beads after treatment. XRD results showed that the material retained its main bulk characteristics: it is a mainly amorphous material with a small amount of quartz (SiO_2), and such a tiny proportion of rutile and anatase that it does not allow quantification with this technique.

Photocatalysis Experiments

Batch Reactor

Irradiation experiments were carried out in a 200 ml open system. The photoreactor consisted of a medium-pressure Hg-vapor Heraeus TQ 150 Z lamp, filtered under 350 nm with a DURAN 50® glass jacket (thermostated at 25°C) and, thus, emitting only near UV–visible (NUV–vis) light, immersed in a cylindrical borosilicate glass reactor (**Scheme 1A**). The photon flux at 366 nm (main emission line), determined by potassium ferrioxalate actinometry (Kuhn et al., 2004), was $2.38 \cdot 10^{-6}$ E s^{-1}. The reactor was covered with aluminum foil to avoid photonic loss and maximize its efficiency through reflection.

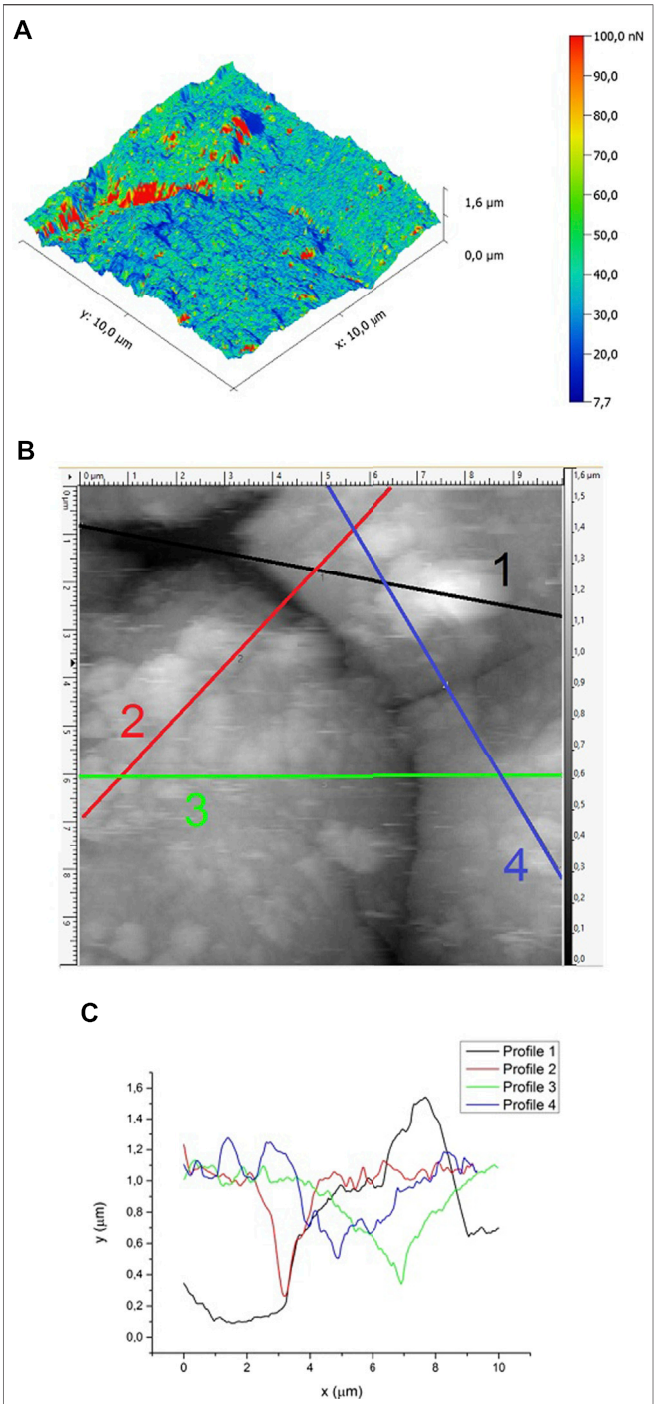

FIGURE 5 | 3D topography of the surface of etched glass beads coated by liquid phase deposition method and calcined at 700°C (LPDe-700). **(A)** 3D topographic map overlaid with adhesion forces, **(B)** top view of this area, also indicating the profiles where **(C)** the cross-section analysis of the deepest holes was performed.

200 ml of 0.01 g L^{-1} phenol solution and 1 g of glass beads coated with a photocatalyst were used in each experiment. Adsorption equilibrium was allowed to be established for 30 min in the dark, without significant spectral changes, and the lamp, previously ignited and warmed up, was inserted in the reactor. The photocatalyst/solution mixture was kept under magnetic stirring (750 rpm) while irradiating for 6.5 h. 1 ml aliquots were withdrawn at different reaction times and immediately centrifuged for 10 min at 14,000 rpm (≡ 17,746 g, enough force even for the settling of TiO_2-P25 nanoparticles), prior to the analysis. Photolysis of phenol in the absence of any photocatalyst, and photodegradation catalyzed by TiO_2 nanoparticles (as TiO_2-P25, 0.1 g in 200 ml), was also carried out for comparative purposes.

TABLE 1 | Average results of quantitative EDS analysis and Si/Ti ratio measured for untreated glass beads and etched glass beads coated by the liquid phase deposition method and calcined at 700°C (LPDe-700).

Material	Weight (%)			Si/Ti
	O	Si	Ti	
Untreated glass beads	41.80	39.55	–	–
LPDe-700	47.78	24.15	15.19	1.59

Flow Reactor

The medium-pressure Hg-vapor lamp was positioned, together with its cooling and filtering glass jacket, in parallel to a horizontal borosilicate glass tube (inner diameter 11.4 mm), where the phenol solution (thermostated to within 25°C) was flowing, propelled by a peristaltic pump from a continuously stirred reservoir (**Scheme 1B**). Both the lamp and the photoreactor tube were placed into a cylindrical aluminum mirror to avoid photonic loss and maximize its efficiency through reflection.

250 ml of 0.01 g L^{-1} phenol solution and 0.5 g of glass beads coated with the photocatalyst were employed in each experiment. These were spread along 6 cm of the inside of the photoreactor tube (same length as the lamp bulb) between two glass wool stoppers (**Figure 2**). The uniform shape of the coated glass beads allowed an arranged distribution of the catalyst to obtain a reproducible irradiated surface between experiments. Upon lamp warming time, phenol solution contained in the reservoir was continuously recirculated through the tube at 0.75 ml s^{-1}, which means that the hydraulic retention time in the tube section containing the photocatalyst was 8.2 s, while irradiating for 6.5 h. Aliquots were collected and analyzed as described below.

Analysis and Characterization

Upon centrifugation, obtained supernatant, free from any photocatalyst particles, was either dark stored in closed vials until HPLC analysis, always performed on the same day, or frozen and HPLC/MS analyzed as soon as possible. No reaction was observed along these periods.

Phenol degradation was monitored by HPLC with a Spectra System (Thermo Fisher) instrument equipped with a photodiode array detector. Chromatographic separation was performed by a C18 Hypersil ODS-2 column (150 × 4.6 mm, 5 µm particles), together with a 1.0 ml min^{-1} isocratic acetonitrile-aqueous (25:75) mobile phase. 50 µL samples were injected, and phenol was detected at 272 nm and 11.5 min retention time.

Photoproducts were identified using HPLC/MS (Thermo Scientific LTQ Orbitrap Discovery apparatus), equipped with

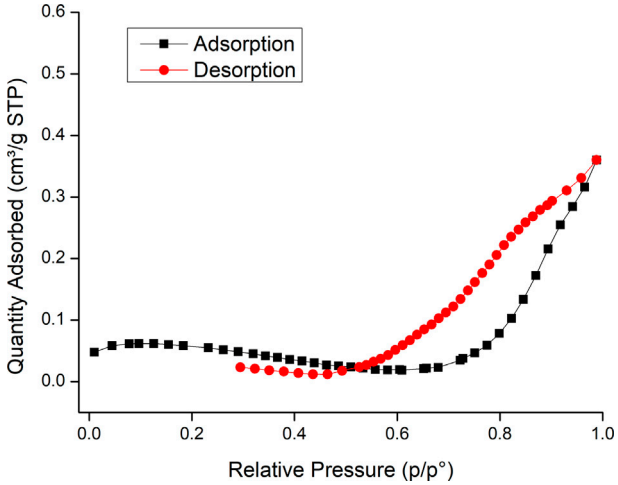

FIGURE 6 | BET isotherm of etched glass beads coated by the liquid phase deposition method and calcined at 700°C (LPDe-700).

an electrospray interface operating in a negative ion mode (ESI-). A Phenomenex Kinetex XB-C18 column (100 × 2.1 mm, 2.6 μm) was used and operated at 30°C with elution solvents A (0.1% formic acid) and B (0.1% methanol) at a flow rate of 200 μL min^{-1}. The gradient was as follows: 0–1 min, 95–95% A, and 5–5% B; 1–8 min, 95–5% A, and 5–95% B; 8–10 min, 5–5% A, and 95–95% B; 10–11 min, 5–95% A, and 95–5% B; 11–15 min, 95–95% A, and 5–5% B. Typical injection volumes were 5–25 μL. The analyses were carried out using full-scan data–dependent MS scanning from m/z 50 to 500.

N_2 adsorption–desorption isotherms were measured by means of a TriStar II Plus (Micrometrics) apparatus, and the surface area was calculated according to BET isotherm. Micrographs of photocatalytic glass beads were taken with a digital microscope. Scanning electron microscopy (SEM) analysis was performed using JSM-6400 (JEOL) equipment. A Siemens D5000 X-ray diffractometer was used for the energy dispersive X-ray spectroscopy (EDXS) quantitative analysis. Mechanical data (topography, stiffness, and adhesion) were measured with a Keysight 9500 atomic force microscopy (AFM) scanning probe, equipped with a 90 μm scanner.

RESULTS AND DISCUSSION

Characterization of the Immobilized Catalysts

The structure and morphology of both the starting glass beads and the coated ones were analyzed by SEM. The glass surface becomes rough upon etching, according to the images obtained (**Figures 1B**, **3**). The etched surface reveals a larger abundance of microcracks and caves than just the cleaned glass, which is in agreement with the formation of a thin nanoporous layer with superhydrophilic properties (Liu et al., 2014). Besides, etching caused quite an apparent color change from transparent to dull white.

Liquid phase deposition on etched glass beads calcined at 700°C (LPDe-700) produced a thin TiO_2 layer fully covered by a network of microcracks (**Figure 4A**), with some regions where the catalyst film was lost by detachment (**Figure 4B**).

The AFM 3D topography of the coating of an LPDe-700 beads sample exhibits a relatively smooth surface with some deep holes, which correspond to a closer image of the microcracks and slight adhesion fluctuation (**Figure 5A**). Here, adhesion is the tendency of two dissimilar materials, TiO_2 and a silicate surface, to cling onto one another. Thus, adhesion would be of dispersive nature, possibly based on the physisorption equilibrium. A top view of this area (**Figure 5B**) shows small plates and hemispherical grains

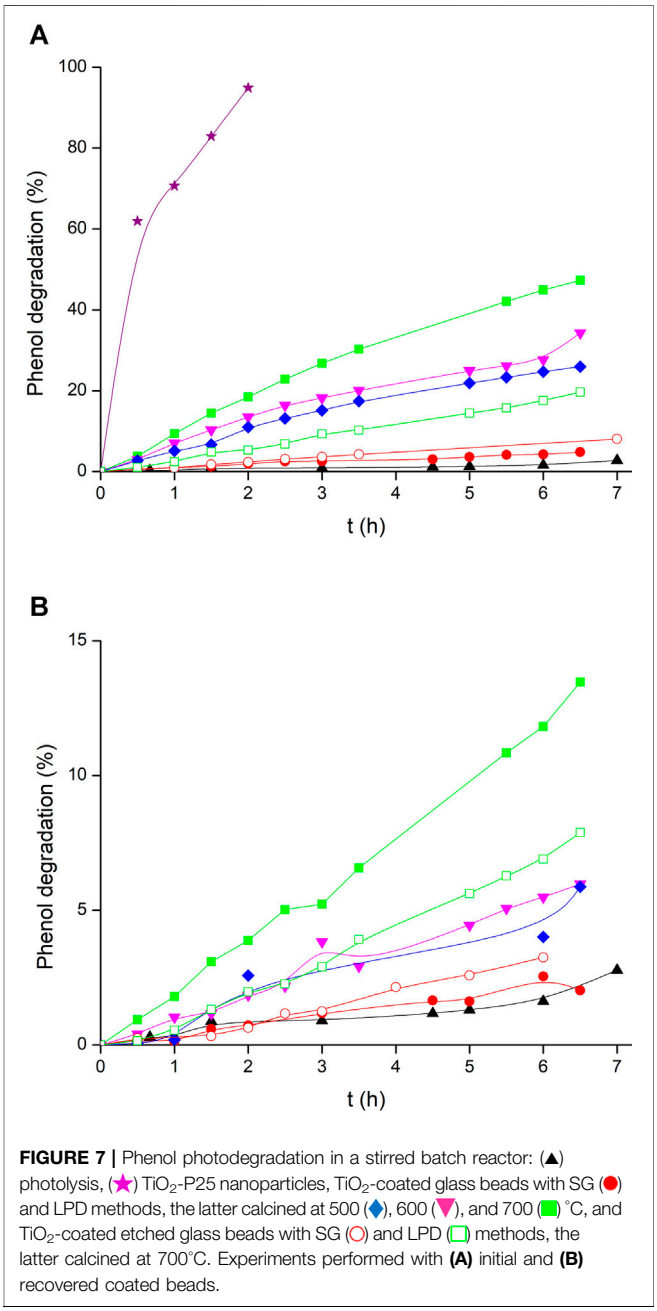

FIGURE 7 | Phenol photodegradation in a stirred batch reactor: (▲) photolysis, (★) TiO_2-P25 nanoparticles, TiO_2-coated glass beads with SG (●) and LPD methods, the latter calcined at 500 (◆), 600 (▼), and 700 (■) °C, and TiO_2-coated etched glass beads with SG (○) and LPD (□) methods, the latter calcined at 700°C. Experiments performed with **(A)** initial and **(B)** recovered coated beads.

TABLE 2 | Observed rate constants for the photocatalytic decomposition of phenol in a stirred batch reactor with TiO_2-coated glass beads, both initial and recovered. SG and LPD stand for the immobilization method, **e** denotes etched material, and, finally, the figures indicate calcination temperature. Remaining activity, calculated as 100 × k_{obs} (Rec.) / k_{obs} (Init.), is a measure of the recoverability of the photocatalyst, here evaluated after one single 6.5 h run.

Material	Initial	Recovered	Remaining activity (%)
	$k_{obs}\cdot10^6$ (s^{-1})	$k_{obs}\cdot10^6$ (s^{-1})	
Stirred batch reactor			
None	0.8 ± 0.1	–	–
TiO_2-P25	375 ± 49	–	–
SG-600	1.9 ± 0.1	1.02 ± 0.08	53
SGe-600	3.40 ± 0.07	1.58 ± 0.08	46
LPD-500	13.0 ± 0.4	2.4 ± 0.4	18
LPD-600	15.7 ± 0.8	2.62 ± 0.05	17
LPD-700	27.6 ± 0.3	6.01 ± 0.16	22
LPDe-700	9.2 ± 0.2	3.6 ± 0.1	39
Flow reactor			
None	10.9 ± 0.3	–	–
LPD-700	29.8 ± 0.3	20.9 ± 0.3	70

combined to make up the structure of the TiO_2 coating; a typical grain width is of the order of 750 nm. A cross-section analysis of the cracks (**Figures 5B,C**) reveals a maximum peak-to-valley height difference of 1.45 μm (profile 1), while the observed deepness of the cracks varies around 0.6–0.8 μm (profiles 2–4). These cracks are deep enough to facilitate that any mechanical aggression to the surface results in film detachment. Also, a comparison of **Figures 5A,B** indicates that the lowest adhesion forces are found along the observed cracks and in the deeper regions of these ones. Thus, continuous mechanical aggression implies an almost complete loss of film coating.

EDXS measurements taken at different points of the coating confirmed the presence of titanium on the TiO_2-coated surface. Most relevant results of the elemental analysis performed on the surface of only cleaned glass beads and coated ones are reported in **Table 1**. EDXS spectra of untreated glass beads did not detect titanium, so its presence on LPDe-700 surface is exclusively related to coating. Several bead samples yielded a similar titanium content (14–15%) indicating that the coating is homogeneous and supporting that the adsorption equilibrium was attained on these surfaces.

The BET surface area was obtained from N_2-adsorption data (**Figure 6**), yielding a value of 0.14 ± 0.01 $m^2\,g^{-1}$ for LPDe-700 glass beads, considerably higher than 0.0092 ± 0.0004 $m^2\,g^{-1}$, reported for non-coated glass beads (Keating, 2014), but much lower than the 50 $m^2\,g^{-1}$ surface measured for nanosized TiO_2-P25 (Canle et al., 2005).

The obtained adsorption isotherm (**Figure 6**) corresponds to Type III according to IUPAC's classification of physisorption isotherms (Thommes et al., 2015). This isotherm does not identify any monolayer formation; typically, it indicates weak adsorbent–adsorbate interactions and clustering of the adsorbed molecules around the most favorable sites on the surface. It can also be an evidence of a macroporous solid where the amount of adsorbate at saturation pressure remains finite. A hysteresis Type H3 loop is featured, which may suggest the presence of nonrigid aggregates of plate-like particles and/or macropores. All this experimental evidence is in good agreement with the observation of lack of mechanical stability.

Photodegradation

Stirred Batch Reactor

Kinetic data obtained for phenol photodegradation in the absence or presence of the studied photocatalysts are depicted in **Figures 7A,B**, and the corresponding rate constants are collected in **Table 2**. Phenol degradation by direct 366 nm photolysis was very slow, yielding a low rate constant with a high standard deviation that may be neglected in comparison with most other cases. For comparison, suspended TiO_2-P25 nanoparticles yielded a much higher rate.

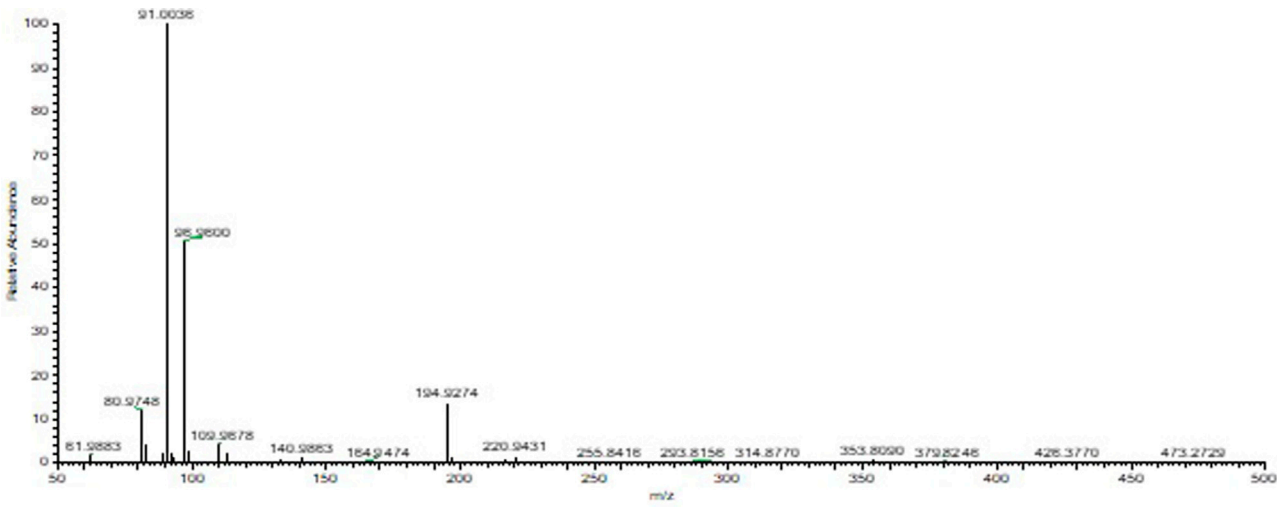

FIGURE 8 | Typical HPLC-MS mass spectrum of phenol photoproducts.

TABLE 3 | HPLC-MS data for all phenol photoproducts observed upon 366 nm radiation with TiO_2-coated glass beads in a stirred batch reactor.

Observed photoproducts	Structure	$[M-H]^-$ (m/z)	Retention time (min)
(1) Pyrocatechol and/or resorcinol and/or hydroquinone	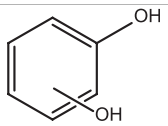	109.9678	1.70
(2) Hexa-2,4-dienedioic acid	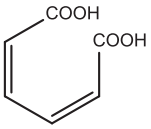	140.9863	1.50
(3) Penta-2,4-dienoic acid	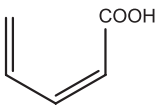	96.9600	1.46
(4) Carbonic acid	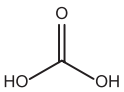	61.9883	1.45
(5) Penta-2,4-dienal	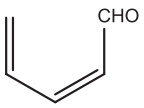	80.9748	1.44
(6) Pent-2-enoic acid	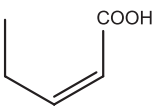	98.9557	1.58
(7) Pent-2-enal	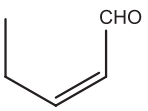	82.9719	1.43
(8) 3-Hydroxypropyl acid	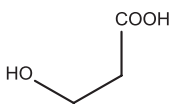	89.0245	1.67
(9) Hex-2-enedioic acid	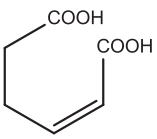	142.9656	1.52
(10) Biphenyl	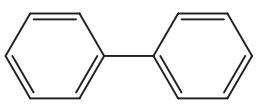	152.9253	1.04
(11) (2-Hydroxyphenyl) (phenyl) methanone	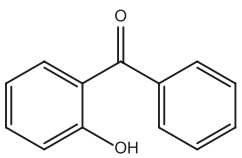	196.9233	1.49
(12) 9H-Xanthen-9-one	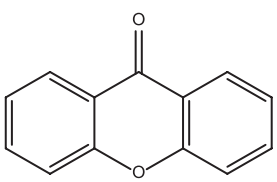	194.9275	1.53

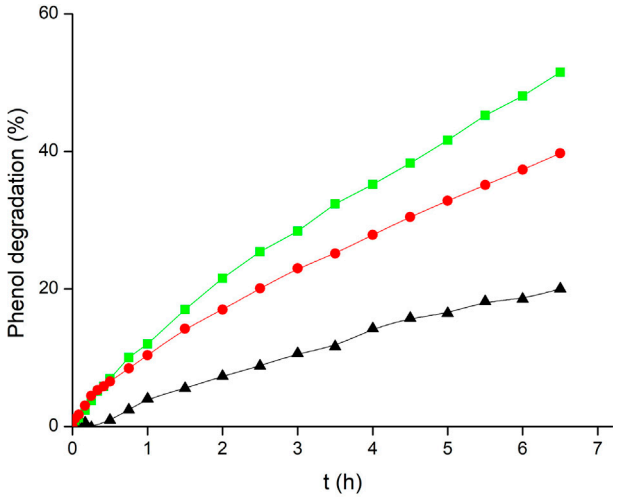

FIGURE 9 | Phenol photodegradation in a flow reactor: (▲) photolysis, TiO_2-coated glass beads with liquid phase deposition method calcined at 700°C (LPD-700): (■) initial and (●) recovered material.

Photodegradation was slow when using SG-coated glass beads, while all LPD beads showed better catalytic activity, which increased with calcination temperature (**Figure 7A**) as has been previously observed (Yu et al., 2003). Etched glass beads were also coated by using both methods SG and LPD, followed by calcination, the latter at 700°C, as this temperature revealed to be more efficient. Etching yielded dissimilar results. While LPDe-700 beads had lower activity than any other unetched LPD catalyst, SG-coated etched glass beads displayed considerably better phenol photodegradation than SG-600 beads, although this method still produces much less effective catalytic coatings than LPD technique. Different hypotheses may be put forward to explain this observation, mainly pointing to changes in the characteristics of the surface: roughness, porosity, heterogeneity, etc. Our preferred working hypothesis is that these different behaviors between etched catalysts, either SG or LPD, may arise from the fact that glass etching produces a microrough surface with superhydrophilicity (Liu et al., 2014), which attracts water better than other less polar species. Thus, in the case of the LPD method, where coating is performed in aqueous solutions, water molecules strongly attach to the nanoporous glass surface, which could prevent the adhesion of TiO_2 particles. However, this is not the case in the SG method, where a mainly ethanol solution is used. Thus, glass etching has a positive effect on coatings performed by SG method while it is unfavorable when used with the LPD method. Anyway, TiO_2-coated glass beads exhibited very low photoactivity compared to TiO_2-P25 nanoparticles in all cases.

The TiO_2-covered glass beads used in photodegradation experiments were recovered and used again in a second run, and the results are shown in **Figure 7B** and **Table 2**. All beads suffered a considerable loss in their photocatalytic activity, so that much slower phototransformation processes were observed. Also, it can be noticed that all these beads lost most of their TiO_2 coating after only two uses in the batch reactor (**Figures 1C,D**), which can explain the decrease in the catalytic activity. SG-coated substrates, both untreated and etched, presented better recoverability, with ca. 50% activity kept in the first repetition after recovery, but the corresponding reaction rates were so low that a quite significant part of the degradation might be just attributed to direct photolysis.

It is remarkable that recoverability in LPD-coated glass beads improves with higher calcination temperatures. This indicates that high-temperature annealing increased the adhesion of the TiO_2 layer, which may be indicative of a transition from physisorption to chemisorption, though this would require further study (Vieira et al., 2016).

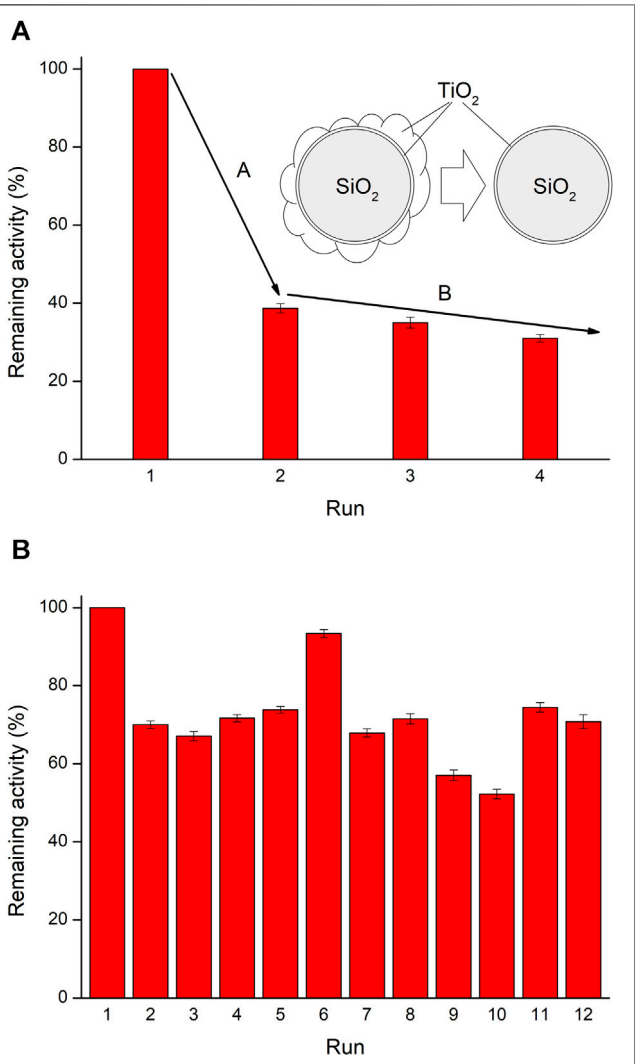

FIGURE 10 | Activity decrease with subsequent recovering cycles for the photocatalytic decomposition of phenol **(A)** in a stirred batch reactor with etched TiO_2-coated glass beads by the liquid phase deposition method and calcined at 700°C (LPDe-700), and **(B)** in a flow reactor with TiO_2-coated glass beads by the liquid phase deposition method and calcined at 700°C (LPD-700). Remaining activity is calculated as 100 × k_{obs} (Rec.) / k_{obs} (Init.).

Furthermore, etching had a great effect on the recoverability of the catalyst, as the recovered beads keep a much higher activity when their glass surface has been etched prior to coating. This implies that the surface microroughness obtained by etching favors adhesion between materials, preventing coating detachment. However, the photodegradation rate in the repeated experiment was still lower than with corresponding unetched beads, as etching already caused a noticeable 3-fold rate decrease in the first-use photocatalytic beads. As previously stated, this can be interpreted as due to a largely increased nanoscale roughness, with more wettability of the etched glass surface, which affects the LPD coating, prepared in an aqueous solution, resulting in less catalyst immobilized on the glass beads.

Identification of photoproducts was carried out by comparison with authentic samples, with results in agreement to those already found and published elsewhere. A typical MS spectrum of the products obtained in the photodegradation is displayed in **Figure 8**, while the identified chemicals are collected in **Table 3**. No new products were found with respect to our previous studies (Boukhatem et al., 2017; Belekbir et al., 2020).

Flow Reactor

Phenol photodegradation was studied in the flow reactor to have a better understanding of the issue of the mechanical stability of the photocatalyst-coated beads. Thus, the photocatalyst that produced the best results in the stirred batch reactor was used: glass beads coated by LPD and calcined at 700°C (LPD-700), and the reaction was also monitored in the absence of any catalyst. On the other hand, the process catalyzed by TiO_2-P25 nanoparticles in the flow reactor was not measured, since the correct use of very small sized catalysts is complex in this kind of systems and their recovery would be even more difficult (which is why, as previously stated, a safe immobilization of catalysts on the surface of bulkier substrates is such an important issue).

The obtained kinetic results, both with freshly coated glass beads and with recovered glass beads, are depicted in **Figure 9**, and the corresponding rate constants collected in **Table 2**. The observed reactions were faster than in the stirred batch reactor, despite the irradiation source was the same and the photocatalyst load (2 g L^{-1}) was lower than in stirred batch reactor experiments (5 g L^{-1}). This corresponds to a 76% rate increase at constant catalyst load after subtracting photolysis (also much faster), which indicates the importance of the geometry of the photoreactor and the photocatalyst arrangement on the kinetics of the reaction. Because of this, any comparison with kinetic data from other studies has not been performed, since there are too many factors affecting the rate, apart from the photocatalyst employed. Besides, remaining activity of recovered LPD-700 beads in this case was much higher than in the stirred reactor (70% *vs* 22%). This difference must arise just from the mechanical peeling of TiO_2-coated glass beads through crashing with the magnetic bar, with the reactor walls and with other beads in the stirred batch reactor, while no crashes, abrasion or collisions take place in the flow reactor, where the phenol solution flowed in a gentle orderly laminar regime (Reynolds number $N_{Re} \approx 100$).

Performance of Recycled Catalysts

Stirred Batch Reactor

Successive reuse of the photocatalysts has been studied with the most promising coated beads: LPDe-700 in stirred batch reactor and LPD-700 in flow reactor. The use of glass beads instead of other smaller and cheaper materials, which could be easily suspended in a batch reactor, has been chosen for their spherical and uniform morphology. These beads allow a similar distribution profile of the photocatalyst in the flow reactor in different experiments. Thus, consecutive measurements are more reproducible, and the results can be better compared without any other interfering factors.

The LPDe-700 catalyst has been recovered and reused three times in the stirred batch reactor (**Figure 10A**). After the first use, the activity reduced sharply, indicating that the most crumbly layer had peeled out. However, the recycled photocatalyst also lost activity in successive runs, though showing a less relevant change, that is, just 10% of activity was lost after each "use and recover" cycle. These recycled beads still kept some catalytic activity, quite reduced with respect to the initial experiment that must be proportional to the amount of catalyst coating remaining on the glass surface. It follows from these results that the photocatalytic beads do not lose their activity regularly after recycling. An initial stage (A) corresponds to an intense peeling of excess TiO_2 from the surface, this process may depend on film hardness and on stirring intensity. This behavior points to the existence of a multilayer coating, with the second and successive physisorbed layers being lost readily and just the first one, more strongly attached to the surface of the glass beads and possibly chemisorbed, remaining. In a second stage (B) the activity reduces more slowly and linearly, possibly in relation to a progressive leaching of the remaining chemisorbed TiO_2. At this step, the adhesion between supported TiO_2 and the glass surface may also affect the process. Again, the fact that activity loss during stage B is slower is an indirect evidence of a stronger chemisorption surface interaction.

Flow Reactor

Results obtained in the flow reactor displayed a very different behavior. The untreated LPD-700 beads were selected for this experiment as they yielded higher degradation rates, despite their catalytic layer seemed weaker than that of the corresponding etched substrate. However, the catalyst could maintain its activity less altered through several cycles in the flow reactor (**Figure 10B**). After each use, the photocatalyst was washed *in situ* with flowing water (1 L) and dried overnight with continuous air flow. The activity loss after the first experiment and recycling (30%) was much larger than in the following runs, as already observed in the stirred batch reactor. Therefore, no significant additional change was obtained in the following two repetitions (runs 3 and 4).

After four repeated degradation experiments and the corresponding cleaning, the catalyst was additionally washed with 1 L of water flowing during 6.5 h while simultaneously receiving the NUV–vis irradiation of the lamp. This method has proven very effective to clean and regenerate the

photocatalyst immobilized on glass beads after degradation of methylene blue (Cunha et al., 2018). The first experiment after NUV–vis regeneration (run 5) showed very similar activity as before but, surprisingly, the second repetition (run 6) was faster and very close to the starting run (only a 7% decrease, perhaps an outlier). Then, the third repetition (run 7) was again slower. A second regeneration cycle was then applied after these seven runs; no rate effect was observed in the first repetition (run 8), but following runs did lose activity, so the third repetition (run 10) only exhibits 52% of the initial activity.

A different regeneration process was tried after these 10 runs. The whole photoreactor, with catalyst in its original place, was rinsed with a flowing mixture of water/acetone (250 ml, 50:50 v/v) followed by washing and drying. Much activity was then recovered in the first repetition (run 11), which may be due to either a better cleaning or a real regeneration of the photoactive surface. The hypothesis of trace amounts of acetone remaining in the system, probably adsorbed on the catalyst and acting as a photosensitizer (Borkman and Kearns, 1966), was ruled out since any adsorbed acetone would be photodegraded during the first measurement (run 11), and then its accelerating effect should not be observed in the second repetition (run 12). However, these last two cycles (runs 11 and 12) yielded very similar reaction rates and, therefore, water/acetone rinsing had a successful effect on the cleaning or regeneration of the catalyst surface, which seems not much damaged after 70 h use in the flow reactor (**Figures 1E,F**), unlike what was observed in the batch reactor in only 13 h (**Figures 1C,D**).

CONCLUSION

LPD is more appropriate than SG for the immobilization of TiO_2 layers on SiO_2 glass surfaces and together with a slow-ramp calcination followed by very slow cooling produces relatively reactive photocatalytic films. Etching of the initial glass surface favors microcracks and caves formation on the surface, resulting in better adhesion of TiO_2. This decreases the friability, thus improving its durability. However, LPD TiO_2-coated etched glass beads exhibit lower photocatalytic activity. The coatings obtained with this method are not homogeneous; a crumbly TiO_2 layer covers a more robust TiO_2 film attached to the glass surface. BET physisorption data and AFM measurements are in agreement with these observations. Even with the best immobilization method, the photocatalyst coating is fragile, and it must be treated carefully when recycling the catalyst for ensuring a long-life activity. We have proved that the use of a flow reactor, with the pollutant solution flowing in a laminar regime through the photocatalyst bed, reduces the abrasion of the photocatalytic surface and its consequent degradation, and increases the durability of the catalytic layer.

DATA AVAILABILITY STATEMENT

The raw data supporting the conclusions of this article will be made available by the authors, without undue reservation.

AUTHOR CONTRIBUTIONS

DRR: experiments, analysis, and writing. MI: experiments, analysis, and writing. MIF: logistics, organization, and supervision. JAS: analysis, writing. MC: concept, organization, supervision, analysis, and writing.

FUNDING

This research was partially supported by the Group React! and funded by the Ministerio de Economía y Competitividad (Spain, Project CTQ2015-71238-R MINECO/FEDER), and by the regional government of the Xunta de Galicia (Spain, Project GPC ED431B 2020/52).

REFERENCES

Alemany, L. J., Bañares, M. A., Pardo, E., Martin, F., Galán-Fereres, M., and Blasco, J. M. (1997). Photodegradation of Phenol in Water Using Silica-Supported Titania Catalysts. *Appl. Catal. B.* 13 (3), 289–297. doi:10.1016/s0926-3373(97)00006-4

Anku, W. W., Mamo, M. A., and Govender, P. P. (2017). "Phenolic Compounds in Water: Sources, Reactivity, Toxicity and Treatment Methods," in *Phenolic Compounds - Natural Sources, Importance and Applications*. Editors M. Soto-Hernandez, M. Palma-Tenango, and M. R. Garcia-Mateos (IntechOpen). doi:10.5772/66927

Belekbir, S., El Azzouzi, M., El Hamidi, A., Rodríguez-Lorenzo, L., Santaballa, J. A., and Canle, M. (2020). Improved Photocatalyzed Degradation of Phenol, as a Model Pollutant, over Metal-Impregnated Nanosized TiO_2. *Nanomaterials* 10 (5), 996. doi:10.3390/nano10050996

Borkman, R. F., and Kearns, D. R. (1966). Triplet-state Energy Transfer in Liquid Solutions. Acetone-Photosensitized Cis-Trans Isomerization of Pentene-2. *J. Am. Chem. Soc.* 88 (15), 3467–3475. doi:10.1021/ja00967a001

Boukhatem, H., Khalaf, H., Djouadi, L., Gonzalez, F. V., Navarro, R. M., Santaballa, J. A., et al. (2017). Photocatalytic Activity of Mont-La (6%)-Cu0.6Cd0.4S Catalyst for Phenol Degradation under Near UV Visible Light Irradiation. *Appl. Catal. B Environ.* 211, 114–125.

Bruce, W., Meek, M. E., and Newhook, R. (2001). Phenol: Hazard Characterization and Exposure-Response Analysis. *J. Environ. Sci. Health C* 19 (1), 305–324. doi:10.1081/gnc-100103589

Calia, A., Lettieri, M., and Masieri, M. (2016). Durability Assessment of Nanostructured TiO_2 Coatings Applied on Limestones to Enhance Building Surface with Self-Cleaning Ability. *Building Environ.* 110, 1–10. doi:10.1016/j.buildenv.2016.09.030

Canle, M. L., Santaballa, J. A., and Vulliet, E. (2005). On the Mechanism of TiO_2-Photocatalyzed Degradation of Aniline Derivatives. *J. Photochem. Photobiol. A. Chem.* 175 (2), 192–200. doi:10.1016/j.jphotochem.2005.05.001

Cao, B., Zhao, J., Yu, Y., Li, W., Xu, S., Sun, R., et al. (2020). High Efficient Hydrogen Evolution over Self-Reproducible Platinum Photocatalyst. *Catal. Today* 340, 183–187. doi:10.1016/j.cattod.2018.09.036

Cunha, D. L., Kuznetsov, A., Achete, C. A., Machado, A. E. d. H., and Marques, M. (2018). Immobilized TiO_2 on Glass Spheres Applied to Heterogeneous Photocatalysis: Photoactivity, Leaching and Regeneration Process. *Peer J.* doi:10.7717/peerj.4464

Ćurković, L., Ljubas, D., Šegota, S., and Bačić, I. (2014). Photocatalytic Degradation of Lissamine Green B Dye by Using Nanostructured Sol–Gel TiO_2 Films. *J. Alloy. Compd.* 604, 309–316.

Dang, T. T. T., Le, S. T. T., Channei, D., Khanitchaidecha, W., and Nakaruk, A. (2016). Photodegradation Mechanisms of Phenol in the Photocatalytic

Process. *Res. Chem. Intermed.* 42 (6), 5961–5974. doi:10.1007/s11164-015-2417-3

Fujima, T., Futakuchi, E., Tomita, T., Orai, Y., and Sunaoshi, T. (2014). Hierarchical Nanoporous Glass with Antireflectivity and Superhydrophilicity by One-Pot Etching. *Langmuir* 30 (48), 14494–14497. doi:10.1021/la502873d

Gartner, M., Scurtu, R., Ghita, A., Zaharescu, M., Modreanu, M., Trapalis, C., et al. (2004). Spectroellipsometric Characterization of Sol-Gel TiO_2-CuO Thin Coatings. *Thin Solid Films* 455-456, 417–421. doi:10.1016/j.tsf.2004.01.030

General Assembly of the United Nations (2015). *Goal 6. Ensure Availability and Sustainable Management of Water and Sanitation for All. Transforming Our World: The 2030 Agenda for Sustainable Development (A/RES/70/1*. New York: United Nations.

Goffredo, G., and Munafò, P. (2015). Preservation of Historical Stone Surfaces by TiO_2 Nanocoatings. *Coatings* 5 (2), 222–231. doi:10.3390/coatings5020222

Gutiérrez-Tauste, D., Domènech, X., Angeles Hernández-Fenollosa, M., and Ayllón, J. A. (2006). Alternative Fluoride Scavengers to Produce TiO_2 Films by the Liquid Phase Deposition (LPD) Technique. *J. Mater. Chem.* 16 (23), 2249–2255. doi:10.1039/b515367k

He, Y., Sutton, N. B., Rijnaarts, H. H. H., and Langenhoff, A. A. M. (2016). Degradation of Pharmaceuticals in Wastewater Using Immobilized TiO_2 Photocatalysis under Simulated Solar Irradiation. *Appl. Catal. B: Environ.* 182, 132–141. doi:10.1016/j.apcatb.2015.09.015

He, Y., Zhu, Y. F., and Yu, F. (2004). TiO_2 Mesoporous Film Photocatalyst Supported on Glass Beads. *J. Inorg. Mater.* 19 (2), 385–390.

Ibukun, O., and Jeong, H. K. (2020). Tailoring Titanium Dioxide by Silver Particles for Photocatalysis. *Curr. Appl. Phys.* 20 (1), 23–28. doi:10.1016/j.cap.2019.10.009

Keating, K. (2014). A Laboratory Study to Determine the Effect of Surface Area and Bead Diameter on NMR Relaxation Rates of Glass Bead Packs. *Near Surf. Geophys.* 12 (2), 243–254. doi:10.3997/1873-0604.2013064

Kim, J.-H., Lee, M. J., Kim, S., Hwang, J., Lim, T.-Y., and Kim, S.-H. (2012). Fabrication of Patterned TiO_2 Thin Film by a Wet Process. *Met. Mater. Int.* 18 (5), 833–837. doi:10.1007/s12540-012-5013-8

Kuhn, H. J., Braslavsky, S. E., and Schmidt, R. (2004). Chemical Actinometry (IUPAC Technical Report). *Pure Appl. Chem.* 76 (12), 2105–2146. doi:10.1351/pac200476122105

Lee, B.-N., Liaw, W.-D., and Lou, J.-C. (1999). Photocatalytic Decolorization of Methylene Blue in Aqueous TiO_2 Suspension. *Environ. Eng. Sci.* 16 (3), 165–175. doi:10.1089/ees.1999.16.165

Liu, H. F., Zheng, B. J., Dao, A. Q., Yi, S. T., Jiang, D. S., Fu, C. Y., et al. (2014). One-pot Synthesis and Photocatalytic Activity of SnO_2/TiO_2 Nanocomposite Thin Film. *Mater. Res. Innov.* 18 (Suppl. 2), S2–S707. doi:10.1179/1432891714z.000000000552

Ma, B., Goh, G. K. L., Ma, J., and White, T. J. (2007). Growth Kinetics and Cracking of Liquid-Phase-Deposited Anatase Films. *J. Electrochem. Soc.* 154 (10), D557. doi:10.1149/1.2769828

Meng, X., Zong, P., Wang, L., Yang, F., Hou, W., Zhang, S., et al. (2020). Au-nanoparticle-supported ZnO as Highly Efficient Photocatalyst for H_2O_2 Production. *Catal. Commun.*

Mikula, M., Brezová, V., Cěppan, M., Pach, L., and Karpinský, Ľ. (1995). Comparison of Photocatalytic Activity of Sol-Gel TiO_2 and P25 TiO_2 Particles Supported on Commercial Fibreglass Fabric. *J. Mater. Sci. Lett.* 14 (9), 615–616. doi:10.1007/bf00586156

Munafò, P., Quagliarini, E., Goffredo, G. B., Bondioli, F., and Licciulli, A. (2014). Durability of Nano-Engineered TiO_2 Self-Cleaning Treatments on limestone. *Construction Building Mater.* 65, 218–231. doi:10.1016/j.conbuildmat.2014.04.112

Osborn, D., Hassan, M., Asadi, S., and White, J. R. (2014). Durability Quantification of TiO_2 Surface Coating on Concrete and Asphalt Pavements. *J. Mater. Civ. Eng.* 26 (2), 331–337. doi:10.1061/(asce)mt.1943-5533.0000816

Parsons, S. (2004). *Advanced Oxidation Processes for Water and Wastewater Treatment*. IWA publishing.

Retamoso, C., Escalona, N., González, M., Barrientos, L., Allende-González, P., Stancovich, S., et al. (2019). Effect of Particle Size on the Photocatalytic Activity of Modified Rutile Sand (TiO_2) for the Discoloration of Methylene Blue in Water. *J. Photochem. Photobiol. A: Chem.* 378, 136–141. doi:10.1016/j.jphotochem.2019.04.021

Senthilkumaar, S., and Porkodi, K. (2005). Heterogeneous Photocatalytic Decomposition of Crystal Violet in UV-Illuminated Sol-Gel Derived Nanocrystalline TiO_2 Suspensions. *J. Colloid Interf. Sci.* 288 (1), 184–189. doi:10.1016/j.jcis.2005.02.066

Shen, C., Wang, Y. J., Xu, J. H., and Luo, G. S. (2016). Oxidative Desulfurization of DBT with H_2O_2 catalysed by TiO_2/Porous Glass. *Green. Chem.* 18 (3), 771–781. doi:10.1039/c5gc01653c

Singh, D., Singh, N., Sharma, S. D., Kant, C., Sharma, C. P., Pandey, R. R., et al. (2011). Bandgap Modification of TiO_2 Sol-Gel Films by Fe and Ni Doping. *J. Sol-gel Sci. Technol.* 58 (1), 269–276. doi:10.1007/s10971-010-2387-2

Štangar, U. L., Černigoj, U., Trebše, P., Maver, K., and Gross, S. (2006). Photocatalytic TiO_2 Coatings: Effect of Substrate and Template. *Monatsh. Chem.* 137 (5), 647–655.

Subba Rao, K. V., Zhuo, B., Cox, J. M., Chiang, K., Brungs, M., and Amal, R. (2006). Photoinduced Bactericidal Properties of Nanocrystalline TiO_2 Thin Films. *J. Biomed. Nanotechnology* 2 (1), 71–73. doi:10.1166/jbn.2006.006

Tasbihi, M., Ngah, C. R., Aziz, N., Mansor, A., Abdullah, A. Z., Teong, L. K., et al. (2007). Lifetime and Regeneration Studies of Various Supported TiO_2 Photocatalysts for the Degradation of Phenol under UV-C Light in a Batch Reactor. *Ind. Eng. Chem. Res.* 46 (26), 9006–9014. doi:10.1021/ie070284x

Thommes, M., Kaneko, K., Neimark, A. V., Olivier, J. P., Rodriguez-Reinoso, F., Rouquerol, J., et al. (2015). Physisorption of Gases, with Special Reference to the Evaluation of Surface Area and Pore Size Distribution (IUPAC Technical Report). *Pure Appl. Chem.* 87 (9-10), 1051–1069. doi:10.1515/pac-2014-1117

Vieira, E. M. F., Ribeiro, J. F., Sousa, R., Silva, M. M., Dupont, L., and Gonçalves, L. M. (2016). Titanium Oxide Adhesion Layer for High Temperature Annealed Si/Si_3N_4/TiO_x/Pt/$LiCoO_2$ Battery Structures. *J. Elec Materi* 45 (2), 910–916. doi:10.1007/s11664-015-4223-5

Wang, X., Chen, A., Chen, B., and Wang, L. (2020). Adsorption of Phenol and Bisphenol A on River Sediments: Effects of Particle Size, Humic Acid, pH and Temperature. *Ecotoxicol. Environ. Saf.* doi:10.1016/j.ecoenv.2020.111093

Wang, X., Li, Z., Shi, J., and Yu, Y. (2014). One-dimensional Titanium Dioxide Nanomaterials: Nanowires, Nanorods, and Nanobelts. *Chem. Rev.* 114 (19), 9346–9384. doi:10.1021/cr400633s

White, G. C. (1986). *The Handbook of Chlorination*. New York: Van Nostrand Reinhold.

Xi, W., and Geissen, S.-u. (2001). Separation of Titanium Dioxide from Photocatalytically Treated Water by Cross-Flow Microfiltration. *Water Res.* 35 (5), 1256–1262. doi:10.1016/s0043-1354(00)00378-x

Xia, Q., Li, Z., Xi, H., and Xu, K. (2005). Activation Energy for Dibenzofuran Desorption from Fe^{3+}/TiO_2 and Ce^{3+}/TiO_2 Photocatalysts Coated onto Glass Fibres. *Adsorption Sci. Tech.* 23 (5), 357–366. doi:10.1260/026361705774355469

Xu, Z.-Y., Luo, Y., Zhang, D.-W., Wang, H., Sun, X.-W., and Li, Z.-T. (2020). Iridium Complex-Linked Porous Organic Polymers for Recyclable, Broad-Scope Photocatalysis of Organic Transformations. *Green. Chem.* 22 (1), 136–143. doi:10.1039/c9gc03688a

Yu, J.-G., Yu, H.-G., Cheng, B., Zhao, X.-J., Yu, J. C., and Ho, W.-K. (2003). The Effect of Calcination Temperature on the Surface Microstructure and Photocatalytic Activity of TiO_2 Thin Films Prepared by Liquid Phase Deposition. *J. Phys. Chem. B.* 107 (50), 13871–13879. doi:10.1021/jp036158y

Zainudin, N. F., Abdullah, A. Z., and Mohamed, A. R. (2010). Characteristics of Supported Nano-TiO_2/ZSM-5/silica Gel (SNTZS): Photocatalytic Degradation of Phenol. *J. Hazard. Mater.* 174 (1), 299–306. doi:10.1016/j.jhazmat.2009.09.051

Conflict of Interest: The authors declare that the research was conducted in the absence of any commercial or financial relationships that could be construed as a potential conflict of interest.

Publisher's Note: All claims expressed in this article are solely those of the authors and do not necessarily represent those of their affiliated organizations, or those of the publisher, the editors and the reviewers. Any product that may be evaluated in this article, or claim that may be made by its manufacturer, is not guaranteed or endorsed by the publisher.